Preprint Title Phenylamino pyrimidine-1,2,3-triazole derivatives as analogs of imatinib: searching for novel compounds against chronic myeloid leukemia

Authors Luiz Claudio F. Pimentel, Lucas V. B. Hoelz, Henayle F. Canzian, Frederico S. C. Branco, Andressa P. de Oliveira, Vinicius R. Campos, Floriano P. S. Júnior, Rafael F. Dantas, Jackson Antônio L. C. Resende, Anna C. Cunha, Nubia Boechat and Mônica M. Bastos

Publication Date 09 Juni 2021

Article Type Full Research Paper

Supporting Information File 1 Supporting+Information_L_Claudio.docx; 7.4 MB

ORCID® iDs Luiz Claudio F. Pimentel - https://orcid.org/0000-0001-7850-3888; Frederico S. C. Branco - https://orcid.org/0000-0002-0863-7087; Vinicius R. Campos - https://orcid.org/0000-0003-3676-5964; Nubia Boechat - https://orcid.org/0000-0003-0146-2218

Phenylamino pyrimidine-1,2,3-triazole derivatives as analogs of imatinib: searching for novel compounds against chronic myeloid leukemia

Luiz Claudio Ferreira Pimentel[1*], Lucas Villas Boas Hoelz[1], Henayle Fernandes Canzian[1], Frederico Silva Castelo Branco[1], Andressa Paula de Oliveira[1], Vinicius Rangel Campos[2], Floriano Paes Silva Júnior[3], Rafael Ferreira Dantas[3], Jackson Antônio Lamounier Camargos Resende[4], Anna Claudia Cunha[2], Nubia Boechat[1], Mônica Macedo Bastos[1]

Address: [1]Laboratorio de Sintese de Farmacos – LASFAR, Fundacao Oswaldo Cruz, Instituto de Tecnologia em Farmacos,, Farmanguinhos – Manguinhos, CEP 21041-250, Rio de Janeiro, Brazil.

[2]Departamento de Química Orgânica, Universidade Federal Fluminense, Campus do Valonguinho, CEP 24020-150, Niterói, Brazil.

[3]Laboratório de Bioquímica Experimental e Computacional de Farmacos, Fundaçao Oswaldo Cruz, Instituto Oswaldo Cruz, CEP 21040-900, Rio de Janeiro, Brazil.

[4]Instituto de Ciências Exatas e da Terra, Universidade Federal de Mato Grosso, Campus Universitário do Araguaia, CEP 78698-000, Pontal do Araguaia, MT, Brazil.

Email: Luiz Claudio Ferreira Pimentel* – luiz.pimentel@far.fiocruz.br

* Corresponding author

Abstract

The enzyme tyrosine kinase Bcr-Abl-1 is the main molecular target in the treatment of chronic myeloid leukemia and can be competitively inhibited by tyrosine kinase inhibitors such as imatinib. New potential competitive inhibitors were synthesized using the phenylamino pyrimidine pyridine (PAPP) group as a pharmacophoric fragment, and these compounds were biologically evaluated. The synthesis of the twelve new compounds was performed in three steps and assisted by microwave irradiation in a 1,3-dipolar cycloaddition to obtain 1,2,3-triazole derivatives substituted on carbon C-4 of the triazole nucleus. All of them had their inhibitory activities evaluated against a chronic myeloid leukemia cell line (K562) that expresses the enzyme tyrosine kinase Bcr-Abl-1 and against healthy cells (WSS-1) to observe their selectivity. Three compounds had promising results, showing an IC_{50} between 1.0 and 7.3 μM, and were subjected to molecular docking studies. This result suggests that such compounds can interact at the same binding site as imatinib, probably sharing a competitive inhibition mechanism. One of them showed the greatest interaction affinity for Bcr-Abl-1 in the docking studies.

Keywords

chronic myeloid leukemia; 1,3-dipolar cycloaddition; imatinib; phenylamino pyrimidine pyridine; 1,2,3-triazole.

Introduction

Changes in tyrosine kinase proteins (TKPs), either by mutation or chromosomal translocation, can turn them into potent oncogenes. Continuity and increased signaling are associated with some types of neoplasms, such as chronic myeloid leukemia (CML) [1].

A CML is a neoplasm of the bone marrow that transforms normal hematopoietic progenitor cells into malignant cells [2]. This transformation is marked by the presence of an acrocentric chromosome known as Philadelphia (Ph). Ph is the result of the reciprocal chromosomal conversion between the proto-oncogene Abl1 of chromosome 9 and the Bcr gene on chromosome 2Å [3,4].

Research activity on compounds able to act as protein tyrosine kinase inhibitors (TKIs), which has intensified since the 1980s, has led to the identification of the phenylamino pyrimidine (PAP) structure [5,6]. The addition of a pyridine ring to the PAP raised its cellular activity, producing phenylamino pyrimidine pyridine (PAPP), which, after some more chemical modifications, culminated in imatinib (IMT) [7]. PAPP has been used to develop new TKIs that are even more potent than IMT, such as nilotinib [6,7]. Such drugs act as inhibitors at the ATP binding site in the inactive form of Bcr-Abl-1, preventing the binding of the protein to ATP in a competitive manner and resulting in the interruption of the substrate phosphorylation process and the transduction of signals; these processes induce cell apoptosis [8,9]. As mutations in the Bcr-Abl-1 enzyme domain can occur, cases of resistance have emerged in treatment with TKIs, compromising its effectiveness [10,11].

By continuing the work that the group has been developing to obtain new imatinib analogs [12-18], in this work, we designed a series of imatinib 1,2,3-triazole analogs **1a-b** and **2a-j** (Figure 1). The choice of a 1,2,3-triazole ring is associated with both

chemical and metabolic stability [19,20] and with the possibility of providing new compounds capable of circumventing resistance in cancer treatment with TKI [21-24]. In this context, the intent is to replace the amide group present in IMT by the 1,2,3-triazole nucleus, similar to compound **3** described in the literature by Li and coworkers [25], as well as to replace the phenyl piperazine group of IMT by homologous groups to generate new derivatives **1a-b**. For compounds **2a-j**, the amide group was maintained, and the 1,2,3-triazole nucleus was added, since the literature demonstrated good results for derivative **4** containing both groups [26]. In addition, the phenyl piperazine group was replaced by different functionalized side chains (Figure 1). It is worth mentioning that compounds 3 and 4 were compared to the reference drug (**IMT**) and differentiated by their close IC_{50} values.

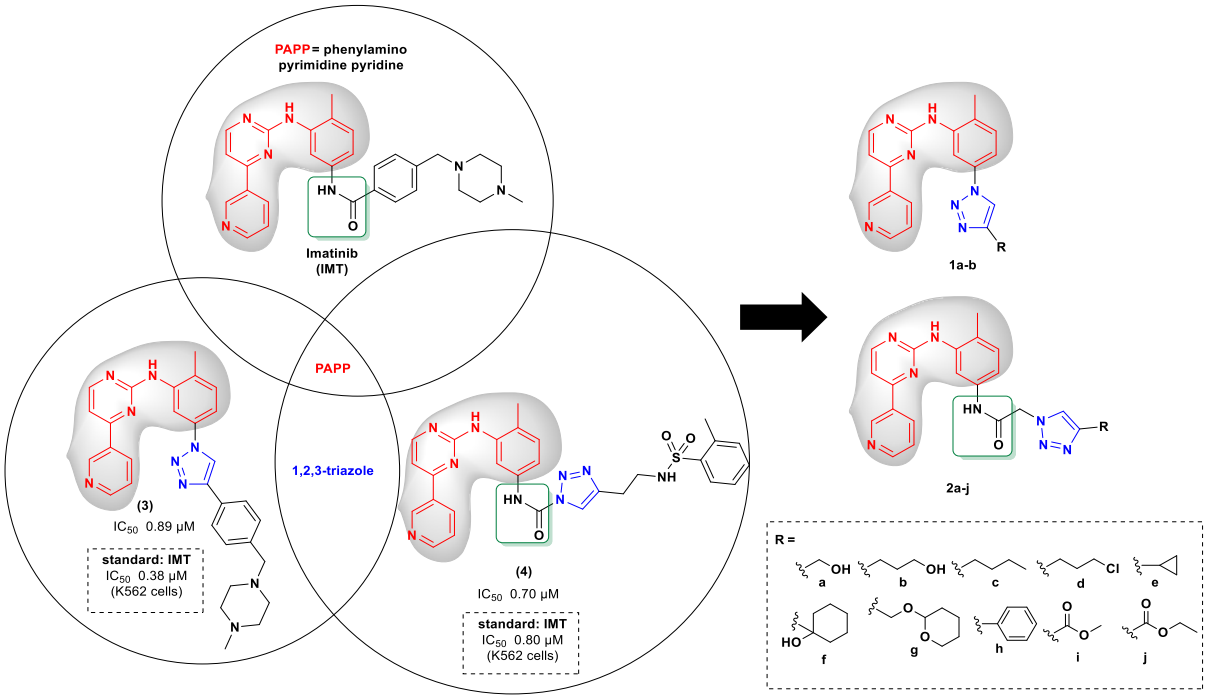

Figure 1. Proposed structural modifications to obtain triazole derivatives **1a-b** and **2a-j**.

All modifications aim to evaluate the influence of the amide group on activity and make a comparison of homologous analogs **1a-b** and **2a-b**. In addition, we expected to verify the different stereoelectronic contributions to biological activity in the replacement of functional groups such as ester **2i-j**, cycloalkanes **2e-f**, saturated heterocycle **2g** and aromatic ring **2h**.

Results and Discussion

Chemistry

Twelve 1,2,3-triazole-1,4-disubstituted IMT derivatives were synthesized (**1a-b** and **2a-j**) (Scheme 1).

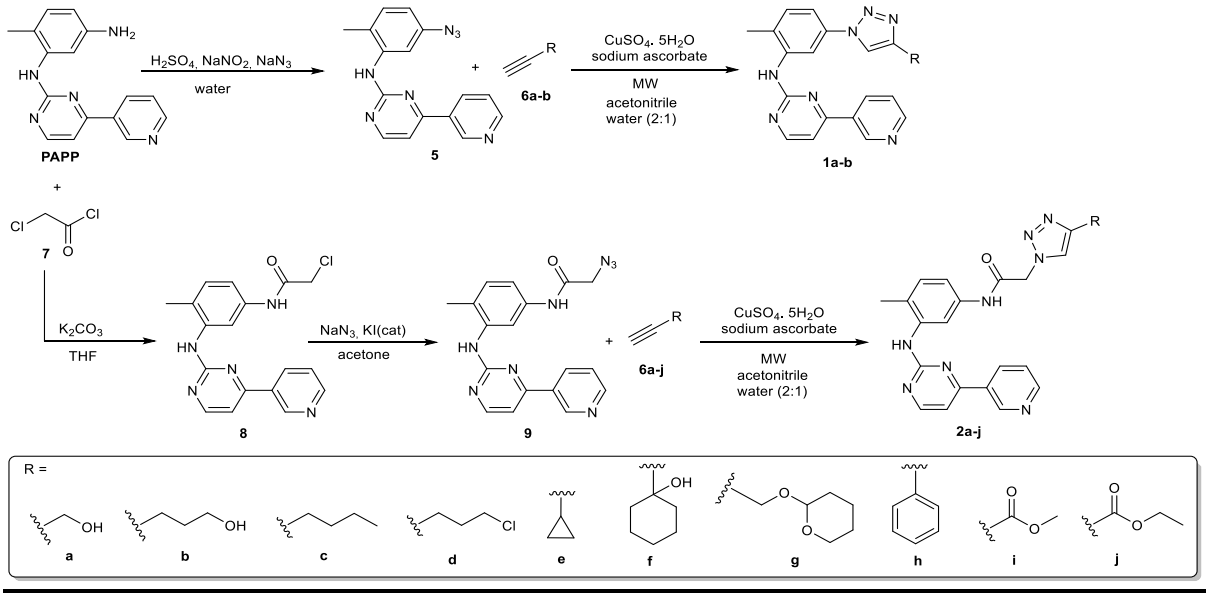

Scheme 1. Synthetic route of the triazole derivatives **1a-b** and **2a-j**.

The compound *N*-(5-azido-2-methylphenyl)-4-(pyridin-3-yl) pyrimidin-2-amine (**5**) was obtained from the aromatic nucleophilic substitution reaction of intermediate PAPP via the formation of a diazonium salt with 84% yield, which was characterized, and its data agreed with those in the literature [27]. The carbonyl nucleophilic substitution

reaction between intermediate **PAPP** and chloroacetyl chloride (**7**) generated the compound chloro-*N*-(4-methyl-3-((4-(pyridin-3-yl)pyrimidin-2-yl)amino)phenyl)acetamide (**8**) in 81% yield, and its characterization data were in accordance with the literature [28]. The compound 2-azido-*N*-(4-methyl-3-((4-(pyridin-3-yl) pyrimidin-2-yl)amino)phenyl)acetamide (**9**) was obtained from the nucleophilic substitution reaction of intermediate **8** in 85% yield. The ^{1}H and ^{13}C NMR spectra of compounds **8** and **9** were similar, but in the IR spectrum of intermediate **9,** it was possible to observe the characteristic stretching of the azide group at 2103 cm^{-1}.

The 1,3-dipolar cycloaddition reactions via copper-catalyzed 1,3-dipolar cycloaddition reaction (CuAAC) of azides **5** and **9** with suitably functionalized acetylenes **8a-j**, using sodium ascorbate and copper sulfate, in ACN/H2O (2:1) under microwave irradiation were carried out to obtain the 1,4-regioisomer of final products **1a-b** and **2a-j**, respectively, with 30-84% yields. This last step was adapted from a method already described in the literature [29].

The formation of compounds **1a-b** and **2a-j** was observed by the disappearance of characteristic stretching of azide groups at 2107 and 2103 cm^{-1} in the IR spectra, which are present in intermediates **5** and **9**, respectively, and compounds **2a-j** showed carbonyl absorption at 1671-1660 cm^{-1} (amide). ^{1}H NMR spectrum analysis showed the appearance of a single signal at 8.52 ppm and between 8.61-7.79 ppm referring to the hydrogen of 1,2,3-triazole (C-5) for compounds **1a-b** and **2a-j**, respectively. In the spectra of ^{13}C NMR, the signals in the range of 165.8–163.5 ppm are attributed to the amide carbonyl in products **2a-j**.

The lower yields in the synthesis of the final products **2a-b** and **2a-j** can be associated with both the difficulty of purifying some products and the high volatility of some acetylenes used, which have been lost at the time of irradiation.

All compounds were obtained with satisfactory purity (>95%) determined by liquid chromatography or elemental analysis. Despite their purity, compounds **2b**, **2d**, **2e** and **2h** had an absence of some signals in the ^{1}H NMR and ^{13}C NMR spectra. For structural confirmation of these new derivatives, we also carried out an X-ray diffraction study of compound **2b**. Yellow single crystals suitable for X-ray diffraction analysis were obtained by slow evaporation of **2b** dichloromethane solution. Based on the X-ray crystallographic analysis, the molecular structure was confirmed, as shown in Figure 2.

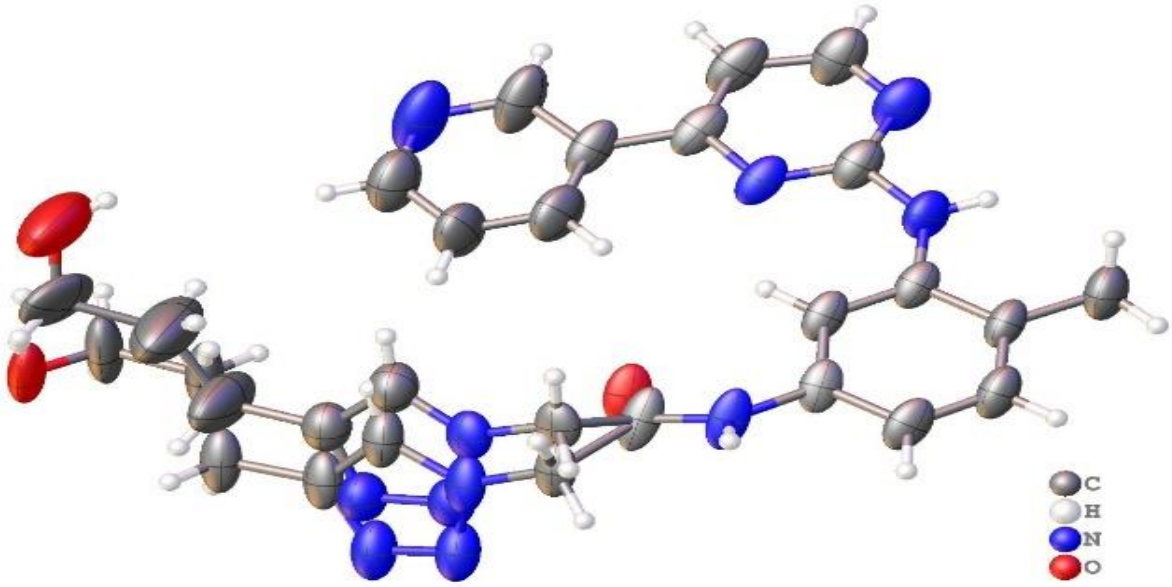

Figure 2. Asymmetric unit representation of the 1,2,3-triazole derivative (**2b**). Displacement ellipsoids are drawn at the 50% probability level.

Biological assay

The compounds showed significant inhibitory activity at 10 μM but not at 1 μM (Figure 3).

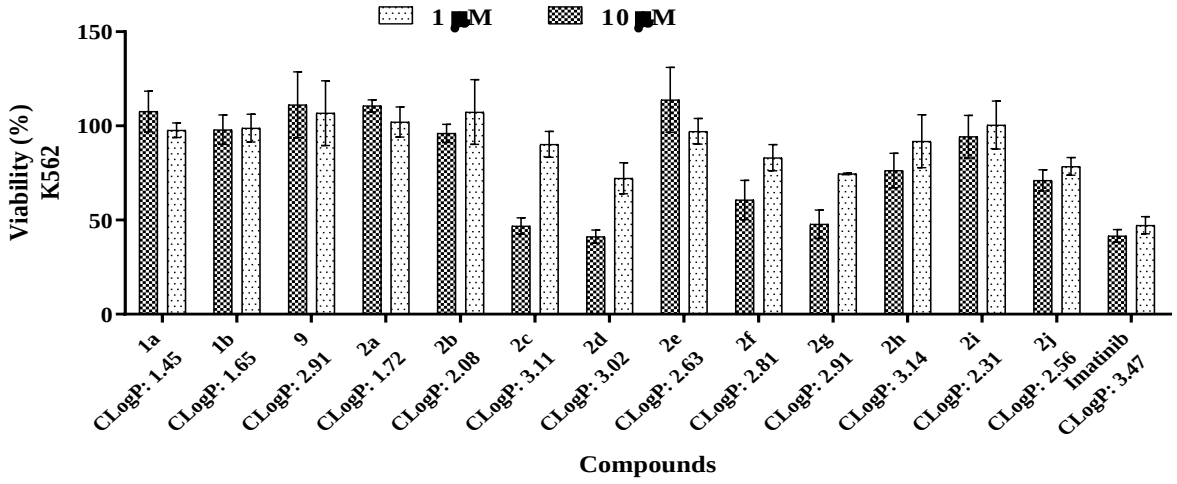

Figure 3. Screening of the triazole derivatives of imatinib **1a-b** and **2a-j** at concentrations of 1 μM and 10 μM against the human cell line K562. Bars represent the mean ± standard deviation. The standard used was IMT.

Compounds **2c-d** and **2g** were the most promising, and concentration-response curves were drawn to determine the cytotoxic concentration (CC_{50}) for 50% of both the K562 and WSS-1 cells so that the selectivity indexes (SIs) could be calculated. These data are shown in Table 1.

Table 1. Cytotoxic activity, confidence interval, and selectivity index of imatinib and derivatives **2c-d** and **2g** against K562 and WSS-1 cell lines.

	CC_{50} (μM)				Selectivity index (SI)[b]
Compound	K562	CI[a]	WSS-1	CI	WSS-1/K562
Imatinib	0.08	0.05 – 0.10	8.9	7.8 – 10.0	111.2
2c	7.3	5.8 – 9.2	6.6	5.7 – 7.6	0.9
2d	1.0	0.8 – 1.3	1.4	1.2 – 1.7	1.4
2g	2.3	1.9 – 2.8	3.9	3.4 – 4.5	1.7

[a] CI: confidence interval (95%)
[b] SI: CC_{50} (WSS-1)/ CC_{50} (cancer cell K562)

Even with a small number of compounds, the structure-activity relationship (SAR) shows that with the exception of compound **2h**, which presents a phenyl ring as a side chain (R), derivatives with aliphatic side chains showed greater toxic activity against K562 cells (Figure 3). One hypothesis is that the derivatives that present higher lipophilicity (**2c**, **2d**, and **2g**) quantified by the octanol-water partition coefficient (cLogP, calculated by ALOGPS) [30] may have better passive diffusion through the membrane of the target cell, increasing its concentration in the intracellular medium and consequently its activity.

When comparing the CC_{50} values of the compounds selected in the cell viability test **2c-d** and **2g** with IMT, used as a positive control, all were less potent against K562 cells and more toxic to WSS-1, with a low SI (Table 1). It is worth mentioning that compounds with low SIs can act as chemotherapeutics [31-33]. Despite being less potent than IMT, derivatives **2c-d** and **2g** were capable of inhibiting K562 cells on a micromolar scale. Thus, these compounds can be used as a prototype for designing new series of substances with greater potency and less toxicity than IMT, with lesser effects for the patient.

Molecular Docking

Validation of the molecular docking protocol was performed through redocking of the IMT complexed to the Bcr-Abl-1 structure (PDB code: 3PYY) [34]. Thus, the predicted mode with the lowest energy presented a MolDock value of -206.022 arbitrary units (a.u.) and a mean-square deviation of 1.68 Å, validating the molecular docking protocol with RMSD values below 2.00 Å [35].

The results, using the validated molecular docking protocol, show that **2c-d** and **2g** interact with Bcr-Abl-1 at the same binding site as IMT but show differences in the

binding modes and with higher values of interaction energy. Compound **2c** presented a MolDock value of -152.993 a.u.. For compound **2d,** the value was -152.127 a.u., and for compound **2g,** it was -167.520 a.u. (Table 2).

Table 2. Summary of the interactions of each inhibitor and imatinib with the tyrosine kinase Bcr-Abl-1 model.

Inhibitors	H-bond energy (a.u.)[a]	Residues (H-bond interaction)	Steric interaction energy by PLP (a.u.) [b]	Residues (steric interactions)	MolDock score (a.u.)
Imatinib	- 8.97	Asp400, Glu305, Met337, Thr334	- 193.66	Asp400, Glu305, Ile379, Met337, Thr334	- 206.02
2c	- 1.31	Asp400, Leu373	-151.68	Asp400, Glu301, Glu305, Ile379, Leu373, Met309, Val308	- 152.99
2d	- 2.19	Asp400, His380, Ile379	- 149.93	Ala399, Asp400, Glu305, His380, Ile312, Leu373, Met309, Phe378, Val318, Val398	- 152.13
2g	- 2.62	Asp400	- 164.90	Ala399, Asp400, Glu305, His380, Ile312, Ile379, Leu317, Lys219	-167.52

[a] Arbitrary units
[b] Piece wise linear potential

Additionally, the analysis of the interactions between IMT and the enzyme Bcr-Abl-1 shows hydrogen bonds with Glu305, Thr334, Met337, and Asp400 (hydrogen bonding energy = -8.97 a.u.) and steric interactions with Glu305, Thr334, Met337, Ile379, and Asp400 (steric binding energy = -193,658 a.u.), in agreement with the

interactions found for IMT in the 3PYY crystal. The analysis of the inhibitor complexes **2c** and **2g** and Bcr-Abl-1 showed interactions similar to those described for IMT (Figure 4 (a)). Thus, compound **2c** presented hydrogen bonding interactions with Asp400 and Leu383 (hydrogen bonding energy of -1.31 a.u.) and steric interactions with Glu301, Glu305, Val308, Met309, Leu373, Ile379, and Asp400 (steric interaction energy = -151.683 a.u.) (Figure 4 (b)). Similarly, compound **2g** showed a hydrogen bonding interaction with Asp400 (hydrogen bonding energy = -2.62 a.u.) and steric interactions with Lys290, Glu305, Ile312, Leu317, Ile379, His380, Ala399, and Asp400 (steric interaction energy = -164,897 a.u.) (Figure 3 (d)), presenting the best overlap with the co-crystalized IMT structure. However, compound **2d** showed hydrogen bonding interactions with Asp400, His380 and Ile379 (hydrogen bonding energy = -2.19 a.u.) and steric interactions with Glu305, Met309, Ile312, Val318, Leu373, Phe378, His380, Val398, Ala399, and Asp400 (steric interaction energy = -149,932 a.u.) (Figure 4 (c)).

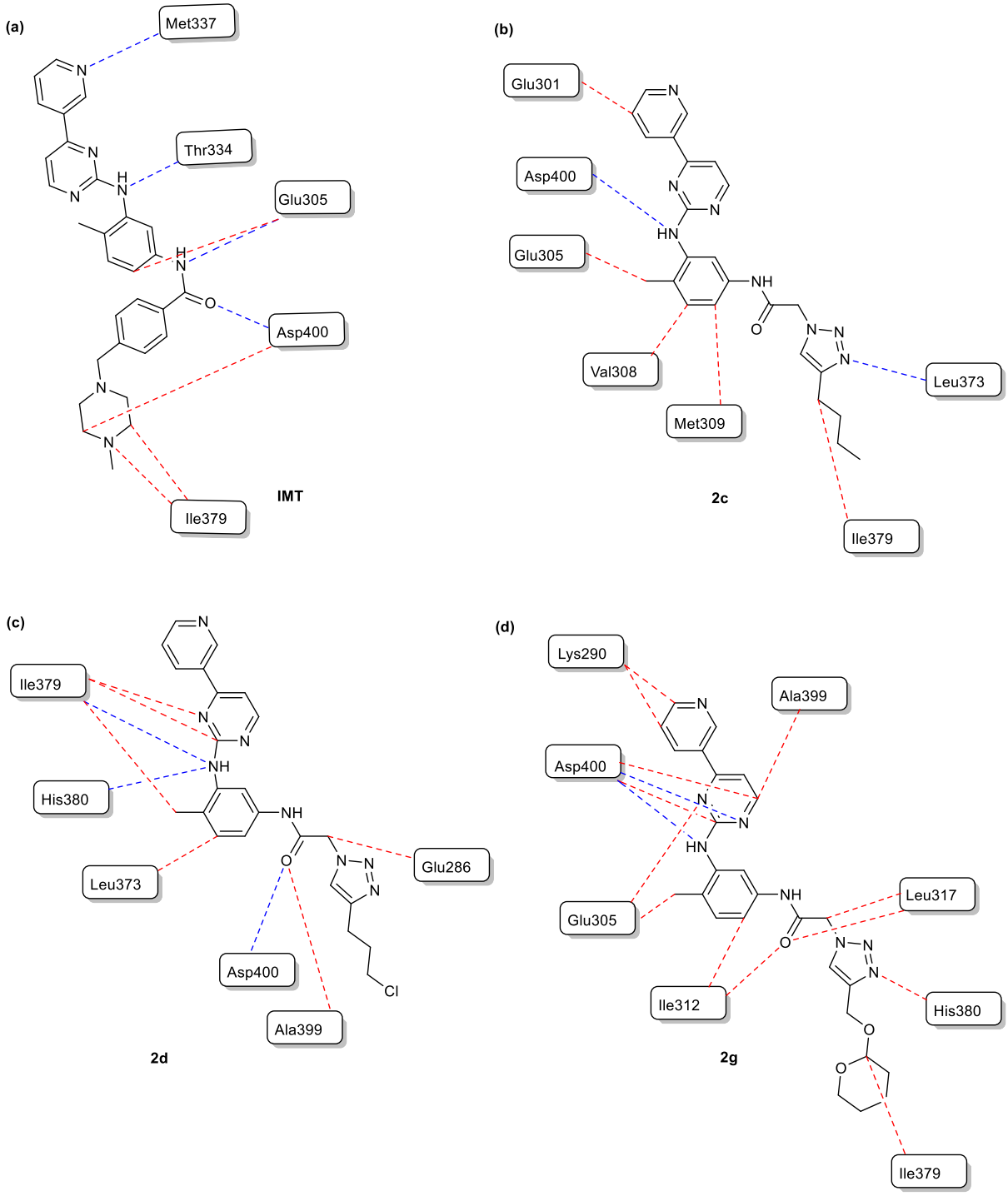

Figure 4. Interaction maps of IMT, **2c-d** and **2g** compounds with the Bcr-Abl-1 structure (PDB code: 3PYY), showing steric interactions (red dotted line) and hydrogen bonds (blue dotted line).

Therefore, the computational simulations suggest that the synthesized compounds interact at the same binding site as the IMT, probably sharing a competitive inhibition

mechanism. The predicted affinity between IMT and this enzyme was higher than the affinities found for compounds **2c-d** and **2g**. Among the newly synthesized derivatives, compound **2g** presented the greatest interaction affinity for Bcr-Abl-1 when compared to compounds **2c** and **2d**, which presented almost equivalent interaction energy values.

Conclusion

A new series of 1,2,3-triazole derivatives of IMT that contain the main pharmacophoric group PAPP has been synthesized and characterized.

All compounds **1a-b** and **2a-j** were evaluated in an *in vitro* cell test; these compounds included intermediate **11** and IMT (reference drug). Three of the compounds, **2c-d** and **2g,** were found to be active, with IC_{50} values between 1.0 and 7.3 μM, while the IC_{50} of the reference compound was 0.08 μM. Molecular docking studies suggested that the synthesized compounds **2c-d** and **2g** interact at the same binding site as IMT, probably sharing a competitive inhibition mechanism. In addition, among the three synthesized derivatives, compound **2g** had the highest interaction affinity for Bcr-Abl-1 when compared to compounds **2c-d**, which presented almost equivalent interaction energy values. However, these results cannot be directly correlated with *in vitro* antimyeloproliferative assessments, which require an enzyme inhibition assay against Bcr-Abl-1.

Experimental

The experimental details and analytical data for intermediates **5**, **8** and **9** and title compounds **1a-b** and **2a-j** were given in Supporting Information File 1. The chemical

structures of all title compounds were confirmed by ^{1}H and ^{13}C NMR spectroscopic analyses and HRMS spectrometric analyses.

X-ray data collection and structure refinement

Single crystal X-ray data for **2b** were collected on a Bruker D8 Venture diffractometer using graphite-monochromated MoKα radiation (λ = 0.71073 Å) at 298 K. Data collection, cell refinement and data reduction were performed with Bruker Instrument Service v4.2.2, APEX2 [36] and SAINT [37], respectively. Absorption correction using equivalent reflections was performed with the SADABS program [38]. The structure solutions and full-matrix least-squares refinements based on F^2 were performed with the SHELX package [38,39] and were refined with fixed individual displacement parameters [Uiso\(H) = 1.2 Ueq (Csp^2 and C_{ar}) or 1.5 U_{eq} (Csp^3)] using a riding model. All nonhydrogen atoms were refined anisotropically. Some crystallization and X-ray diffraction experiments for compound **2b** were performed. All samples evaluated had low scattering patterns and germinated crystals. This resulted in poor quality data, which limited the quality of the refinement. Structure illustrations were generated using ORTEP-3 for Mercury [40], and crystallographic tables were constructed using Olex2 [41]. X-ray crystallographic data in cif format are available at CCDC 2073131 can be obtained free of charge via www.ccdc.cam.ac.uk/data_request/cif.

Crystal Data of 2b

$C_{23}H_{24}N_8O_2$ (*M* = 444.50 g/mol): monoclinic, space group $P2_1/c$, *a* = 14.895(3) Å, *b* = 16.167(3) Å, *c* = 9.5274(14) Å, *β* = 92.150(5)°, *V* = 2292.7(7) $Å^3$, *Z* = 4, *T* = 298.0 K, μ(MoKα) = 0.087 mm^{-1}, F (000) = 936.0, Crystal size = 0.24 x 0.22 x

0.096 mm^3, *Dcalc* = 1.288 g/cm^3; of the 21431 reflections measured (3.72° ≤ 2Θ ≤ 50.682°), 4199 were unique (R_{int} = 0.1422, R_{sigma} = 0.0980) and were used in all calculations. The final R_1 was 0.1284 (I >2σ(I)), and wR_2 was 0.3858 (all data).

Cell line and cell culture

All novel compounds synthesized (**1a-b** and **2a-j**) were evaluated against K562 cells (ATCC® CRL-243TM), a CML cell line, and a WSS-1 healthy cell line (ATCC® CRL-2029TM). The K562 strain was grown in RPMI-1640 medium according to the provider's recommendations [42,43]. Cultivation of WSS-1 cells was performed in DMEM high glucose medium (Vitrocell) according to ATCC recommendations. The media were supplemented with 10% fetal bovine serum (FBS) and 50 mg/MI of the antibiotic gentamicin, and all cell lines were grown in a cell culture bottle, which had a 0.22 µm pore membrane filter on the lid, allowing the circulation of CO_2. WSS-1 cells grew adherently, while cells of the K562 strain grew in suspension. All strains were maintained at 35 °C, at 5% CO_2.

Cell viability assay

WSS-1 cells were incubated at 5 x 10^4 (cells per well) in black plates with a 96-well transparent bottom (Greiner Bio-One) for approximately 20 hours to allow for cell growth and adhesion. The compounds obtained were added at concentrations of 1 µM and 10 µM in DMSO and incubated for 46 hours. This assay was performed in triplicate and measured using resazurin (Sigma-Aldrich) at a concentration of 0.1 mg/mL using a FlexStation 3 microplate reader (Molecular Devices).

K562 cells assay

After plating ($2x10^4$ cell/ml), the K562 cells were incubated for one hour, and then the compounds dissolved in DMSO (Sigma-Aldrich) were added and further incubated for 47 hours. After this period, resazurin was added at a final concentration per well of 0.01 mg/mL, and the first fluorescence reading was immediately performed (λex = 560 nm; λex = 590 nm) (time zero) using FlexStation 3 microplates (Molecular Devices). After the first reading, the plate was returned to the incubator, and after one hour, the second reading was performed, completing the 48 hours of incubation with the compounds. The reference inhibitor used was IMT at fixed concentrations of 1 μM and 10 μM.

Molecular Docking

The Molegro Virtual Docker v6.0 (MVD) program was used to predict the complexes and energies of interaction between the enzyme Bcr-Abl 1 and inhibitors **2c-d** and **2 g**. The crystallographic structures of the enzyme Bcr-Abl-1, complexed with IMT, were extracted from the Protein Data Bank (PDB code: 3PYY) [44]. The structures of the compounds were constructed and optimized by the semi-empirical Recife Model 1 (RM1) method using the Spartan´14 program (Wavefunction, Inc.).

Validation of the molecular docking protocol was performed through the redocking of IMT complexed with the Bcr-Abl-1 structure (PDB code: 3PYY), free of water molecules and cofactors, using Molegro Virtual Docker 6.0 (MVD) [38]. Thus, the whole enzyme was set as the center of the search space. Additionally, the search algorithm MolDock optimizer was used with a minimum of 200 runs, and the parameter settings were as follows: population size = 300; maximum iteration = 2000; scaling factor = 0.50; offspring scheme = Scheme 1; termination scheme = variance-based; crossover

rate = 0.90. Due to the stochastic nature of the algorithm search, ten independent simulations per ligand were performed to predict the binding mode. Consequently, the complexes with the lowest interaction energy were evaluated. The interactions between Bcr-Abl-1 and each inhibitor were analyzed using the ligand map algorithm, a standard algorithm in the MVD program [45]. The usual threshold values for H-bonds and steric interactions were used. All figures for molecular docking results were edited using the Visual Molecular Dynamics 1.9.3 (VMD) program (available for download at http://www.ks.uiuc.edu/Research/vmd/vmd-1.9.3/).

Supporting Information

Supporting information text

Supporting Information File 1:

Additional experimental and analytical data, and NMR spectra of synthesized compounds.

Funding

The author Nubia Boechat thanks the National Council for Scientific and Technological Development – CNPq for recipient of the research productivity fellowship (306193/2018-3) and Monica Macedo Bastos for the fund PROEP (407844/2017-1). They also thank the Fundacao de Amparo a Pesquisa do Estado do Rio de Janeiro – FAPERJ for the fellowship for funding the research of Nubia Boechat (CNE-FAPERJ E-26/202.805/2017). This study was financed in part by the

Coordenacao de Aperfeiçoamento de Pessoal de Nivel Superior - Brazil (CAPES) - Finance Code 001 for PhD student APOs.

References

1. Geary, C. G. *Brit. J. Haematol.* **2000**, *110*, 2-11.

2. Azevedo, L. D.; Bastos, M. M.; Oliveira, A. P. *Quim Nova* **2017**, *40*(7), 791-809.

3. Burnmeister, T.; Schwartz, S.; Bartram, C. R.; Gökbuget, N.; Hoelzer, D.; Thiel, E. *Blood* **2008**, *112*(3), 918-919.

4. Jabbour, E.; Kantarjian, H. *Am. J. Hematol*. **2018**, *93*, 442-459.

5. Yaish, P.; Gazit, A.; Gilon, C.; Levitzki, A. *Science* **1988**, *242*(4880), 933-935.

6. Zhang, Q.; Zhang, X.; You, Q. *Molecules* **2016**, *21*(7), E879.

7. Rossari, F.; Minutolo, F.; Orciuolo, E. *J. Hemat. Oncol.* **2018**, *11*(84), 1-14.

8. Rodriguez, M.; Cardona, A. F.; Grajales, M. A.; Enciso, L.; Ruiz, G.; Yepes, A.; Ospina, V.; Gálvez, K.; García, J.; Rosales, J.; Rosales, M.; Quintero, G.; Rosales, C.; Timana, J. L.; Casas, C. P.; Combariza, J. F.; Vargas, E.; Molano, A. *Rev. Venez. Oncol.* **2007**, *19*(4), 287-296.

9. Kannaiayan, R.; Mahadevan, D. A. *Expert Rev. Anticanc*. **2018**, *18*(12), 1249-1270.

10. Alves, R. C. S. *Rev. Bras. Hematol. Hemoter.* **2009**, *31*(3), 166-177.

11. Hochhaus, A.; Larson, R. A.; Guilhot, F.; Radich, J. P.; Branford, S.; Hughes, T. P.; Baccarani, M.; Deininger, M. W.; Cervantes, F.; Fujihara, S.; Ortmann, C. E.; Menssen, H. D.; Kantarjian, H.; O'brien, S. G.; Druker, B. J. *New Engl. J. Med*. **2017**, *376*(10), 917-927.

12. Bastos, M. M.; Maia, R. C. Compostos derivados de fenilaminopirimidinas processo de obtenção, uso dos ditos compostos, Brazil BR1020140198083; 2014.

13. Boechat, N. Compostos Derivados de fenilamino-pirimidina processo de preparação e uso na terapia da leucemia mieloide crônica. Brazil BR1020140198033; 2014.

14. Boechat, N.; Bastos, M. M.; Maia, R. C. Phenylaminopyrimidine-derived compounds, method for producing the same, use of said compounds for the treatment of cancer, and treatment methods. European Patent Office Germany 15831693.5-1451; 2015.

15. Boechat, N. A.; Bastos, M. M.; Maia, R. C. Phenylaminopyrimidine-derived compounds, method for producing the same, use of said compounds for the treatment of cancer, and treatment methods. WIPO WO2016023090; 2016.

16. Boechat, N.; Bastos, M. M.; Maia, R. C. Phenylaminopyrimidine-derived compounds, method for obtaining, using said compounds in the treatment of cancer, and treatment methods. European Patent Office EP158316935; 2017.

17. Bastos, M. M.; Maia, R. C. Phenylaminopyrimidine-derived compounds, method for producing the same, use of said compounds for the treatment of cancer, and treatment methods. Local Chinese Bureau 201580043231.3; 2017.

18. Azevedo, L. D.; Bastos, M. M.; Vasconcelos, F. C.; Hoelz, L. V. B.; Junior, F. P.S.; Dantas, R. F.; de Almeida, A. C. M.; de Oliveira, A. P.; Gomes, L. C.; Maia, R. C.; Boechat, N. *Med. Chem. Res*. **2017**, *26*, 2929-2941.

19. Dheer, D.; Singh, V.; Shankar, R. *Bioorg. Chem.* **2017**, *71*, 30-54.

20. Bozorov, K.; Zhao, J.; Aisa, H. A. *Bioorg. Med. Chem.* **2019**, *27*(16), 3511-3531.

21. Yang, H.; Yan, R.; Jiang, Y.; Yang, Z.; Zhang, X.; Zhou, M.; Wu, X.; Zhang, T.; Zhang, J. *Eur. J. Med. Res.* **2020**, *187*(111996): 1-13.

22. Banerji, B.; Chandrasekhar, K.; Sreenath, K.; Roy, S.; Nag, S.; Saha, K. D. *ACS Omega* **2018**, *3*(11), 16134-16142.

23. Lee, S. M.; Yoon, K. B.; Lee, H. J.; Kim, J.; Chung, Y. K.; Cho, W. J.; Mukai, C.; Choi, S.; Kang, K. W.; Han, S. Y.; Ko, H.; Kim, Y. C. *Bioorg. Med. Chem.* **2016**, *24*(21), 5036-5046.

24. Zhou, C. H.; Wang, Y. *Curr. Med. Chem.* **2012**, *19*, 239-280.

25. Li, Y. T.; Wang, J. H.; Pan, C. W.; Meng, F. F.; Chu, X. Q.; Ding, Y. H.; Qu, W. Z.; Li, H. Y.; Yang, C.; Zhang, Q.; Bai, C. G.; Chen, Y. *Bioorg. Med. Chem. Lett.* **2016**, *26*(5), 1419-1427.

26. Kalesh, K. A.; Liu, K.; Yao, S. Q. *Org. Biomol. Chem.* **2009**, *7*(24), 5129-5136.

27. Boechat, N.; Bastos, M. M.; Duarte, S. L.; Costa, J. C. S.; Mafra, J. C. M.; Daniel, L. C. C. *RVq* **2013**, *5*(2), 222-234.

28. Yeon, K. D.; Jim, C. D.; Yeol, L. G.; Yeop, K. H.; Hun, W. S.; Fon, L. H.; Mu, K. S.; Am, C. Isothiocyanate compound containing N-phenylpyrimidin-2-amine moiety and method for the preparation thereof. Repub. Korean Kongkae Taeho Kongbo, 2012052095, 2012.

29. Moorhouse, A. D.; Moses, J. E. *Synlett* **2008**, *14*, 2089-2092.

30. Tetko, I. V.; Tanchuk, V. Y. *J. ChemInfComputSci.* **2002**, *42*(5), 1136-1145.

31. Singh, K.; Gangrade, A.; Jana, A.; Mandal, B. B.; Das N. *ACS Omega* **2019**, *4*, 835−841.

32. Badisa, R. B.; Darling-reed, S. F.; Joseph, P.; Cooperwood, J. S.; Latinwo, L. M.; Goodman, C. B. *Anticancer Res.* **2009**, *29,* 2993−2996.

33. Saftić, D.; Žinić, B.; Obrovac, L. G.; Studzińska, M.; Paradowska, E.; Leśnikowski, Z. J. *NucleosNucleot Nucln.* **2018**, *37*(7), 397-414.

34. Yang, J.; Campobasso, N.; Biju, M. P.; Fisher, K.; Pan, X. Q.; Cotton, J.; Galbraith, S.; Ho, T.; Zhang, H.; Hong, X.; Ward, P.; Hofmann, G.; Siegfried, B.; Zappacosta, F.; Washio, Y.; Cao, P.; Qu, J.; Bertrand, S.; Wang, D. Y.; Head, M. S.; Li, H.; Moores, S.;

Lai, Z.; Johanson, K.; Burton, G.; Miller, C. E.; Simpson, G.; Tummino, P.; Copeland, R. A.; Oliff, A. *Chem. Biol.* **2011**, *18*(2), 177-186.

35. Wagner, J. R.; Churas, C. P.; Shuai, L.; Swift, R. V.; Chiu, M.; Shao, C.; Feher, V. A.; Burley, S. K.; Gilson, M. K.; Rommie, E.; Amaro, R. E. *Structure* **2019**, *27*, 1326-1335

36. BRUKER APEX2 v2014.5-0, Bruker AXS Inc., Madison, Wisconsin, USA, 2007.

37. SAINT V8.34A, Bruker AXS Inc., Madison, Wisconsin, USA, 2013.

38. Sheldrick, G. M. SADABS: Program for Empirical Absorption Correction of Area Detector Data, University of Göttingen, Germany. 1996.

39. Sheldrick, G. M. *Acta Crystallogr. A Found Adv.* **2015**, *71*, 3–8.

40. Sheldrick, G. M. *Acta Crystallogr. C Struct. Chem.* **2015**, *71*(1), 3–8.

41. Macrae, C. F.; Edgington, P. R.; McCabe, P.; Pidcock, E.; Shields, G. P.; Taylor, R.; Towler, M.; Streek, J. V. *J. Appl. Crystallogr*. **2006**, *39*, 453–457.

41. Dolomanov, O. V.; Bourhis, L. J.; Gildea, R. J.; Howard, J. A. K.; Puschmann, H. *J. Appl. Cryst.* **2009**, *42*, 339–341.

42. Meng, X.; Li, M.; Wang, X.; Wang, Y.; Ma, D. *Cancer Sci.* **2009**, *100*(6), 1040–1046.

43. Beaufort, A. J.; Bakker, A. C.; Tol, M. J. D.; Poorthuis, B. J.; Scharma, A. J.; Berger, H. M. *Pedriatr. Res.* **2003**, *54*(4), 491–495.

44. Thomsen, R.; Christensen, M. H. *J. Med. Chem.* **2006**, *49,* 3315–3321.